ELSEVIER

Biochemical Pharmacology 63 (2002) 1717–1724

Biochemical Pharmacology

Role of the C-terminus and the long cytoplasmic loop in reduced folate carrier expression and function

Iraida G. Sharina[1], Rongbao Zhao, Yanhua Wang, Solomon Babani, I. David Goldman*

Departments of Medicine and Molecular Pharmacology, Albert Einstein Cancer Center, Albert Einstein College of Medicine, Chanin Two, 1300 Morris Park Ave., Bronx, NY 10461, USA

Received 13 June 2001; accepted 15 November 2001

Abstract

The reduced folate carrier (RFC1), a member of the major facilitative superfamily, generates uphill transport of folates into cells through an exchange mechanism with intracellular organic anions. RFC1 has twelve transmembrane domains with N- and C-termini, and the long loop connecting the 6th and 7th transmembrane domains, directed to the cytoplasm. To elucidate the role of the C-terminus and the long cytoplasmic loop in carrier function, mutants with deletion of the entire C-terminus or with progressive deletions of the loop region were constructed and stably transfected into the murine MTX^rA cell line, which lacks functional RFC1. While expression of the C-terminus-deleted RFC1 protein could not be detected in the cell lysate, the RFC1 mutant lacking 57 of 66 amino acid residues of the long cytoplasmic loop appeared to be inserted into the cytoplasmic membrane but was not functional. In cell lines in which 17 or 31 amino acids were deleted from the carboxyl half of the loop, there was partial preservation of methotrexate, 5-formyltetrahydrofolate, and 5-methyltetrahydrofolate transport. The loss of 5-formyltetrahydrofolate transport activity in the Δ31 and Δ17 mutants was due primarily to a decrease in substrate binding to the carrier. Mutants with partially truncated internal loops demonstrated an anion responsiveness similar to that of wild-type RFC1, indicating that this region of the carrier does not contain a site(s) that plays a role in anion exchange. This is the first study to describe the important role of the long cytoplasmic loop in substrate binding and the crucial role of the C-terminus in maintaining stability of RFC1. © 2002 Published by Elsevier Science Inc.

Keywords: Reduced folate carrier; Cytoplasmic loop; C-terminus; Facilitative transporter; Methotrexate; Deletion

1. Introduction

RFC1 mediates the transport of folate and antifolate compounds in mammalian cells [1]. Based on hydropathy analysis and topological studies, the predicted secondary structure of the RFC1 consists of twelve alpha helical TMDs divided into two equal halves by a long cytoplasmic loop connecting the 6th and 7th TMDs. This loop, along with the N- and C-termini, are predicted to reside within the cytoplasm [2,3]. RFC1 is a member of the MFS of transport carriers, a widely distributed group of polypeptide transporters that mediate translocation of diverse solutes [4]. MFS transporters are inherently equilibrating, but achieve uphill transport in some cases when linked to transmembrane gradients of other compounds that are actively transported by independent mechanisms. RFC1 generates uphill folate transport through an exchange mechanism linked to organic anions, in particular, the high levels of organic phosphates concentrated within the intracellular compartment [5–7].

This laboratory recently initiated a systematic analysis of RFC1 regions and amino acid residues that play an important role in carrier function, particularly as determinants of the selectivity of transport among different folate cofactors and antifolates. These and other studies have identified the first as well as other TMDs as critical to substrate binding and/or the rate of translocation of the carrier–substrate complex [8–15]. Using site-directed and chemical mutagenesis, arginine and lysine residues within TMDs have been indicated recently as important elements

* Corresponding author. Tel.: +1-718-430-2302; fax: +1-718-430-8550.
E-mail address: igoldman@aecom.yu.edu (I.D. Goldman).
[1] Present address: Department of Integrative Biology and the Institute of Molecular Medicine, University of Texas, Houston, TX, USA.

Abbreviations: RFC1, reduced folate carrier; MFS, major facilitative superfamily; 5-CHO-THF, 5-formyltetrahydrofolate; 5-CH_3-THF, 5-methyltetrahydrofolate; MTX, methotrexate; TMD, transmembrane domain; PCR, polymerase chain reaction; HBS, HEPES-buffered saline.

0006-2952/02/$ – see front matter © 2002 Published by Elsevier Science Inc.
PII: S0006-2952(02)00955-3

in RFC1 function [16,17]. In this paper, we explore the role of the C-terminus and the long cytoplasmic loop in RFC1 function and demonstrate that RFC1 transport is highly sensitive to the structural integrity of these regions.

2. Materials and methods

2.1. Chemicals

[3′,5′,7-^{3}H](6*S*)-5-CHO-THF and [3′,5′,7-^{3}H](6*S*)-5-CH_3-THF were obtained from Moravek Biochemicals, and [3′,5′,7-^{3}H]MTX was obtained from the Amersham Corp. Folates were purified by high performance liquid chromatography prior to use [18]. Unlabeled (6*R*,*S*)-5-CHO-THF and (6*R*,*S*)-5-CH_3-THF were used to adjust the specific activity of tritiated compounds for transport studies. All other reagents were of the highest purity available from various commercial sources.

2.2. Construction of plasmids

Deletions were generated by PCR, and in all of the PCR reactions the pPGK-RFC1 plasmid [10] was used as a template. To generate the C-terminal deletion of RFC1, the following nucleotides were used for the PCR reaction: 5′-GCGGATCCACCATGGTGCCCACTGGCCAGGTG-3′ (*Bam*HI) and 5′-GCCTCGAGTCACAGCCCCGCCCAGGCAAAGCAG-3′ (*Xho*I), which contained the *Bam*HI and *Xho*I sites (underlined), respectively. The PCR fragment was digested with *Bam*HI/*Xho*I restriction enzymes and subcloned into the pcDNA3.1 expression vector (Invitrogen). To generate deletions in the internal loop, the C-terminal fragment containing nucleotide residues 801–1539 of RFC1 cDNA was generated by PCR, using the following oligonucleotides as primers, and then cloned into pcDNA3.1 at *Eco*RI/*Xho*I sites: 5′-CGGAATTCCGTCTCTGGTGCCTCTGGTGGGTC-3′ (*Eco*RI) and 5′-GCCTCGAGTCAAGCCTTGGCTTCGAC-3′ (*Xho*I). The N-terminal halves of the internal loop deletants were generated by PCR using the *Bam*HI-containing oligonucleotide (indicated above) as the upstream primer and the following nucleotides as downstream primers: 5′-CGGAATTCGCTCCGCTTAGGGCGCTTTAG-3′ (*Eco*RI), 5′-CGGAATTCTGGCCGGTCAGGCCCCGGGTG-3′ (*Eco*RI), 5′-CGGAATTCGTCCCTGCAAGTGCCCAGCAT-3′ (*Eco*RI).

These fragments were subcloned into pcDNA3.1 containing the C-terminal half of RFC1 at the *Bam*HI/*Eco*RI sites. The PCR products contained nucleotide sequences coding for amino acids 1–621 (Δ57 mutant), 1–705 (Δ31 mutant), or 1–744 (Δ17 mutant). The *Eco*RI linker, used for the generation of internal loop deletions, introduced glutamate and phenylalanine in the location of the deletion. The changes in the coding region for RFC1 were confirmed by automated sequencing of the final constructs.

2.3. Cell culture conditions and generation of cell lines

Cells were grown in RPMI 1640 medium containing 2.3 μM folic acid, supplemented with 10% bovine calf serum (HyClone), 2 mM glutamine, 20 μM 2-mercaptoethanol, 100 units/mL of penicillin, and 100 μg/mL of streptomycin. All cell lines containing mutant RFC1 were obtained by transfection of the MTX^{r}A cell line, which lacks a functional carrier, with DNA plasmids containing deletional RFC1 mutants as reported previously [10]. Briefly, 1×10^7 MTX^{r}A cells were electroporated (300 V, 800 μF) with 40 μg of circular plasmid and selected in RPMI 1640 medium containing 750 μg/mL of G418. Lines were isolated by subsequent cloning on soft agar plates [19].

2.4. Northern analyses

Total RNA was isolated using TRIzol reagent (Life Technologies, Inc.), and 30 μg of RNA was fractionated by electrophoresis on 1% formaldehyde-agarose gels. Transfer and hybridization were performed as described previously [10].

2.5. Western blot analysis

Two polyclonal antibodies, AE390 directed to the distal C-terminus of the murine RFC1 (Met^{499} through Ala^{512}), and AE370 directed to the loop (Asp^{232} through Asp^{248}), were used to probe both total cell lysate and plasma membranes as reported [20]. For total lysate preparation, 3×10^7 cells were harvested, washed twice with HBS (20 mM HEPES, 140 mM NaCl, 5 mM KCl, 2 mM $MgCl_2$, 5 mM glucose, pH 7.4, at 0°) and suspended in 100 μL of the same buffer containing 10 μL of protease inhibitor (P-8340, Sigma). The cell suspension was sonicated for 20 s in a tube submerged in ice water. Plasma membranes were extracted as reported, except that a protease inhibitor cocktail (see above) at a dilution of 1–1000 was used instead of 1 mM phenylmethylsulfonyl fluoride [21]. Protein concentrations of the total lysate and plasma membranes were determined with the BCA Protein Assay Kit (Pierce). Proteins were dissolved in an SDS–PAGE loading buffer [60 mM Tris, 10% glycerol (v/v), 2% SDS, and trace bromophenol, pH 6.8] without heating and resolved on a 12% SDS–polyacrylamide gel. Proteins were transferred to PVDF Transfer Membranes and processed by the ECL Plus western blotting detection system, both obtained from Amersham.

2.6. Transport studies

Influx measurements were performed by a method described previously [22] with minor modifications. The cells were harvested, washed twice with HBS, and resuspended in HBS to 1.5×10^7 cells/mL. Cell suspensions were incubated at 37° for 25 min, uptake was initiated by the

addition of [^{3}H]MTX, [^{3}H]5-CHO-THF or [^{3}H]5-CH_3-THF, and samples were taken at the indicated times. Uptake was terminated by the injection of 1 mL of cell suspension into 9 mL of ice-cold HBS buffer. Cells were collected by centrifugation (1000 *g* for 2 min at 4°), washed twice with ice-cold HBS, and processed to determine intracellular tritium [22]. For all influx measurements, uptake intervals were adjusted to ensure that unidirectional uptake was sustained. For studies that assessed the effect of extracellular Cl^- on MTX influx, HBS was replaced with a HEPES buffer with the same final osmolarity containing 190 mM HEPES, 5 mM glucose, 5 mM KCl, 2 mM $MgCl_2$, pH 7.4.

2.7. MTX cytotoxicity

Cells grown in 96-well plates (1×10^5 cells/mL) were exposed continuously to appropriate concentrations of MTX. After 72 hr, cell numbers were determined by hemocytometer count, and viability was assessed by trypan blue exclusion.

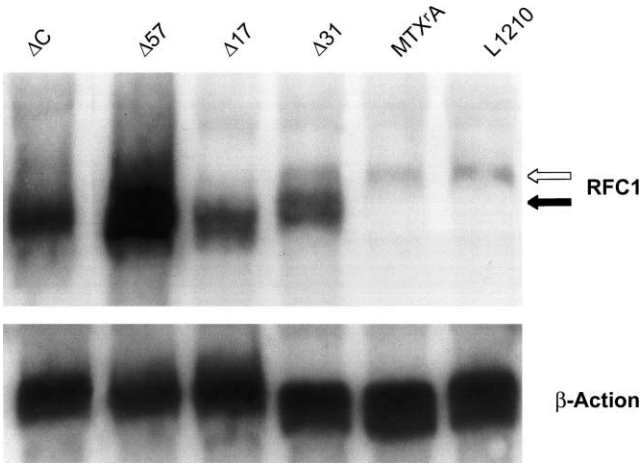

Fig. 2. Northern blot analyses of total RNA. RNA was probed with full-length RFC1 and β-actin cDNAs. Endogenous and transformed RFC1 transcripts are indicated by open and closed arrows, respectively. The picture shown is a representative X-ray film. The level of transcripts was also quantitated by PhosphorImager analysis of radioactive blots and normalized to the levels of β-actin mRNA. The values presented in the text were the average of two such analyses.

3. Results

3.1. Mutagenesis and cell line generation

Clustal alignment [23] of the region between the 6th and the 7th TMDs of rodent and human RFC1 revealed several areas of substantial homology (Fig. 1, underlined). One of the longer of these regions (from position 223–231 of murine RFC1) is located in the N-terminal half of the loop. Three constructs were generated in which 17 (from 249 to 265), 31 (from 235 to 265), and 57 (from 209 to 265) amino acid residues were deleted. Ten amino acid residues were preserved in the largest deletion in an attempt to maintain the proper domain structure. To evaluate the functional importance of the C-terminus, residues starting from position 445 to 512 (last residue of murine RFC1) were deleted; this eliminated all amino acids beyond the predicted 12th TMD.

These constructs were transfected into MTX^{r}A cells, an L1210 murine leukemia cell line derivative with marked impairment of RFC1 function due to an alanine to proline substitution at amino acid 130 in the third TMD [10]. Transfection of pΔ17, pΔ31, pΔ57, and the pΔC-terminus deletion constructs produced stable cell lines identified as Δ17, Δ31, Δ57, and ΔC. RFC1 mRNA in the clonal lines selected for study (Fig. 2) was quantified by PhosphorImager analysis and normalized to the levels of β-actin mRNA. The levels of mutated RFC1 cDNA in Δ17 and Δ31 cells were 2-fold greater than the wild-type RFC1 level in L1210 cells. In the Δ57 and ΔC transfectants, there was 16.5- and 5.6-fold greater expression of mutated RFC1 transcript relative to L1210 cells, respectively.

The expression and localization of truncated RFC1 proteins were evaluated by western analysis with two murine peptide RFC1 antibodies directed to amino acid residues 232–248 (loop) or 499–512 (C-terminus). As indicated in Fig. 3, expression of RFC1 in the recipient MTX^{r}A cells was lower than in L1210 cells. Three dilutions of R16, a line with marked overexpression of RFC1 [10], were used to demonstrate the relationship between signal and the amount of RFC1 loaded on the SDS–polyacrylamide gel. There was a marked increase in protein expression in Δ57 cell lysate as compared with the L1210 cells when the antibody against the C-terminus was

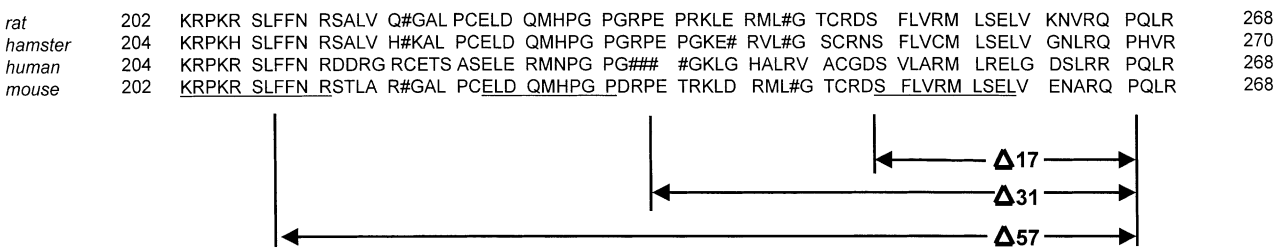

Fig. 1. Protein sequence alignment of the internal loop of the RFC1 from different species. Clustal alignment is shown for the region encompassing the long cytoplasmic loop separating the 6th to 7th TMDs. Areas where there is a high degree of sequence homology are underlined. Double-headed arrows show the locations of deletions generated. The symbol "#" indicates space.

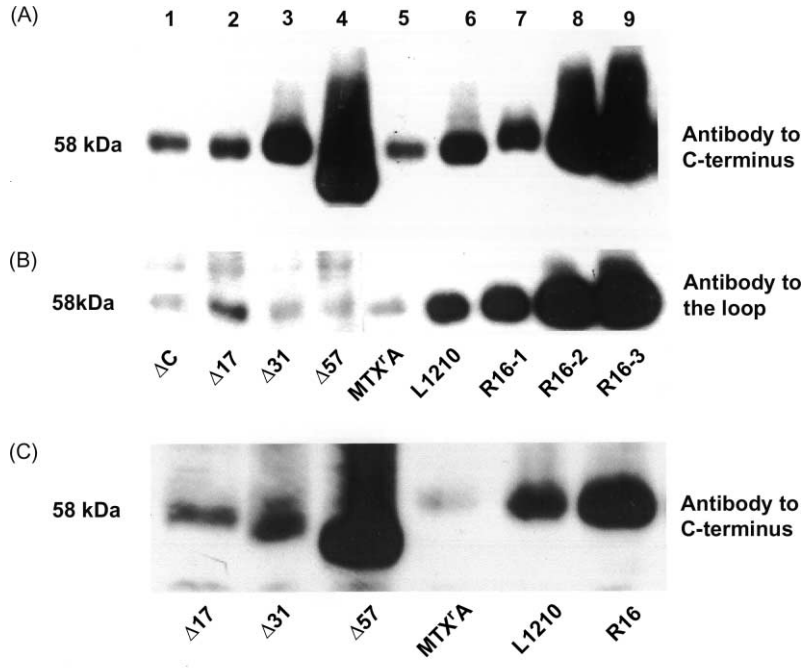

Fig. 3. Western blot analysis of RFC1 expression in transfectants. (A) Total lysates were probed with an antibody directed to the very end of the C-terminus of murine RFC1. Ten micrograms of protein was loaded on lanes 1 through 6, while 0.75, 1.5, and 3 μg of protein were loaded on lanes 7, 8, and 9, respectively. (B) The same amount of total lysate was loaded in each lane as in panel A. However, the blots were probed with an antibody against the loop connecting the 6th and 7th TMDs. (C) Plasma membrane fractions isolated from transfectants were probed with antibody directed to the C-terminus of the protein. Six micrograms of membrane protein was loaded for Δ17, Δ31, Δ57, and L1210 cells, 10 μg for MTX^{r}A cells, and 1.5 μg for R16 cells. The data shown are representative of two experiments.

used (Fig. 3A). Increases in protein expression for Δ31, and to some extent Δ17, deletions also were detectable in comparison to MTX^{r}A cells. There was no difference in the RFC1-specific signal observed with antibodies to the loop between the MTX^{r}A and ΔC cell lines (Fig. 3B), despite a significant increase in ΔC RFC1 mRNA (Fig. 2). Expression of RFC1 in Δ31 and Δ57 cells was comparable to the MTX^{r}A line with the loop antibody since the epitope of this antibody was absent in the transfected truncated proteins. In contrast, RFC1 expression in Δ17 cells was detected with the loop antibody at a level greater than in the recipient MTX^{r}A cells. To determine if the truncated proteins were inserted into the plasma membrane, cell membrane fractions of Δ17, Δ31, and Δ57 cells were prepared and probed with the antibody directed to the C-terminus (Fig. 3C). All these truncated carriers, with the expected trend in reductions in molecular weight, were found in the plasma membrane. The amounts of protein in the membrane fractions reflected the amounts of proteins found in total lysate (Fig. 3A).

3.2. Influx properties

The transfected lines were examined for their capacity to mediate influx of MTX, 5-CHO-THF, and 5-CH_3-THF (Table 1). Influx of all these folates in Δ57 and ΔC transfectants was not different from the levels observed in MTX^{r}A cells. On the other hand, MTX influx in Δ17 and Δ31 cells was ∼23% that of L1210 cells, explained in part by the lower level of carrier expression relative to wild-type L1210 cells (Fig. 3C). Influx of 5-CHO-THF in Δ31 cells was higher than in Δ17 cells. Residual 5-CH_3-THF influx in both lines as compared with L1210 cells was less than that of MTX.

Further studies were undertaken to assess the kinetic basis for the changes in function of the mutant carriers by measuring the influx K_i for 5-CHO-THF using Dixon analysis based upon the assumption that inhibition of [^{3}H]MTX influx by 5-CHO-THF is competitive (Fig. 4). The 5-CHO-THF influx K_i in the Δ17 cells was 35 ± 2.6 μM, or about 6-fold greater than the influx K_i in L1210 cells (5.6 ± 0.8 μM). The influx K_i in Δ31 cells was about half that of Δ17 cells, or 15.6 ± 3.3 μM (based upon the mean ± SEM of three experiments). When these values are compared to the decline in influx of 5-CHO-THF in Δ17 (7-fold) and Δ31 (4-fold) cells (Table 1), it can be seen that the decrease in 5-CHO-THF binding to the RFC1 appears to account for most of the loss of transport activity in Δ17 cells and at least half of the loss of activity in Δ31 cells.

3.3. Impact of the loop deletions on the inhibitory effects of anions on MTX influx

RFC1 functions as an anion exchanger; a variety of inorganic and organic anions act as competitive inhibitors

Table 1
Analysis of influx of MTX, 5-CHO-THF, and 5-CH_3-THF

Cell line	MTX influx (nmol/g dry wt./min)	%[a]	5-CHO-THF influx (nmol/g dry wt./min)	%[a]	5-CH_3-THF (nmol/g dry wt./min)	%[a]
L1210	0.90 ± 0.01	100	2.08 ± 0.19	100	206 ± 0.04	100
Δ17	0.22 ± 0.03	24	0.30 ± 0.09	14	0.18 ± 0.05	8.7
Δ31	0.21 ± 0.01	23	0.58 ± 0.04[*]	28	0.29 ± 0.08[*]	14
MTX^rA	0.050 ± 0.01	5.5	0.049 ± 0.006	2.4	0.061 ± 0.002	3.0
Δ57	0.049 ± 0.002	5.4	0.049 ± 0.006	2.4	0.045 ± 0.005	2.1
ΔC	0.059 ± 0.011	6.5	0.065 ± 0.004	3.1	0.0691 ± 0.005	3.3

Initial uptake rates were measured at an extracellular folate level of 1 μM. Data are the means ± SEM of three experiments.
[a] Relative to L1210 cells.
[*] The difference in influx of 5-CHO-THF between Δ31 and Δ17 cell lines was $P = 0.04$. The difference in 5-CH_3-THF influx between these two lines was $P = 0.28$.

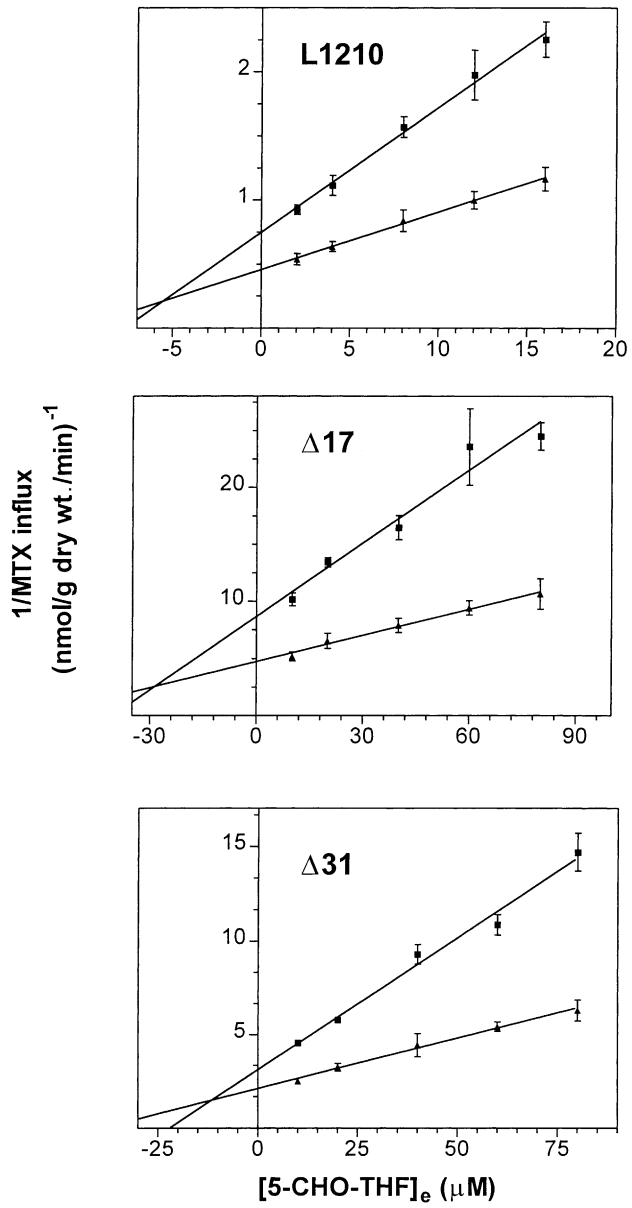

Fig. 4. Determination of 5-CHO-THF influx K_i. After 25 min of incubation in HBS buffer at 37°, uptake was initiated by the addition to the cell suspension of [^{3}H]MTX to achieve concentrations of 1 μM (■) or 2 μM (▲), along with different concentrations of nonlabeled 5-CHO-THF, and incubation was continued for 2 min. K_i values were determined from a Dixon analysis. Data are the averages ± SEM from three separate experiments.

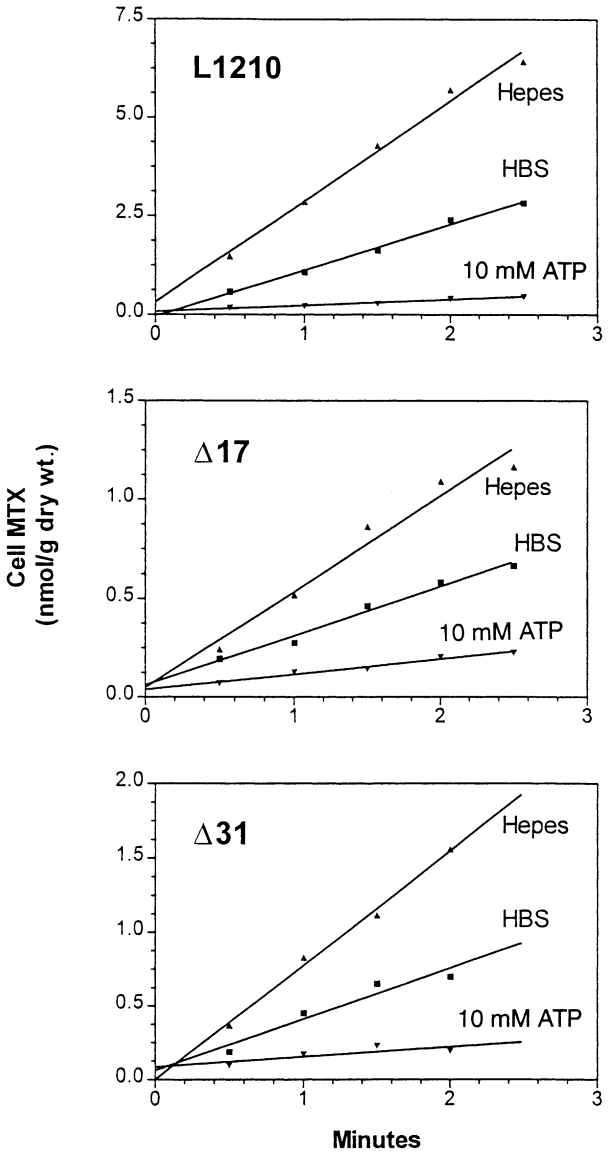

Fig. 5. Effect of buffer anionic composition on MTX influx. Cells were harvested, washed, and re-suspended in HBS, or a buffer in which sodium chloride was isosmotically replaced by HEPES, as described in "Materials and methods." ATP was added to a final concentration of 10 mM simultaneously with the [^{3}H]MTX. Cells were exposed to 1 μM [^{3}H]MTX at time zero, and samples of the cell suspension were taken for cell MTX determinations. Results shown are representative of three separate experiments.

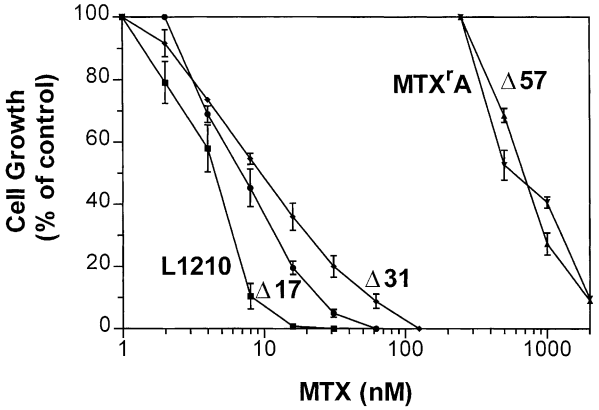

Fig. 6. Growth inhibition by MTX. Cells (2×10^4) were grown in RPMI 1640 medium and exposed to different concentrations of MTX for 72 hr in 96-well plates after which cell numbers were determined by hemocytometer count. Data are the averages ± SEM of three separate experiments.

of influx, and removal of chloride from the extracellular compartment enhances the influx process [5,6]. To evaluate whether the interactions between anions and MTX might involve regions of the long cytoplasmic loop deleted in the RFC1 mutants, the inhibitory effect of 10 mM ATP and the stimulatory effect of chloride removal from the buffer were assessed. As indicated in Fig. 5 (representative of three experiments), the addition of ATP produced inhibitory effects, and the removal of chloride yielded stimulatory effects in the Δ17 and Δ31 cell lines that were not significantly different ($P > 0.5$) from those in L1210 cells.

3.4. MTX cytotoxicity in cell lines with RFC1 long cytoplasmic loop deletions

An important measure of transport function is the capacity of the mutant RFC1s to restore the pharmacologic activity of MTX to a cell line resistant to the drug due to the loss of carrier activity. As indicated in Fig. 6, expression of the Δ57 mutant in the MTX^{r}A cell line had no effect on the MTX IC_{50} value, consistent with the absence of any transport function, as indicated in Table 1. Both the Δ17 and Δ31 cell lines displayed an increase in MTX cytotoxicity with an IC_{50} value nearly two orders of magnitude lower than that of MTX^{r}A cells and only about twice that of L1210 cells. Hence, one-fourth of the MTX transport activity of wild-type cells, mediated by the Δ17 and Δ31 truncated protein lines (see Table 1), was sufficient to sustain near wild-type levels of MTX cytotoxic activity.

4. Discussion

The folic acid family of compounds, in particular 5-CH_3-THF, the major circulating reduced folate in the blood of humans and rodents, are critical to the *de novo* synthesis of purines, pyrimidines, and *S*-adenosylmethionine. Mammals cannot synthesize folates, and hence their absorption *via* the gastrointestinal tract, and subsequent transport into peripheral cells, is essential. The critical role of RFC1-mediated folate transport in mouse development was demonstrated recently by inactivation of RFC1 in mice by homologous recombination [24]. The RFC1-null embryos ceased development before gestation day 9.5, but some embryos could be rescued by maternal folic acid supplementation. However, all RFC1-null neonatal mice died from failure of hematopoietic organs within 12 days [24]. RFC1-mediated transport is also a major determinant of MTX activity, and loss of transport function is an important element in clinical antifolate resistance [25,26]. Hence, there has been considerable interest in the mechanisms by which folates and antifolates are transported into cells [1,27].

RFC1 has many of the characteristics of the MFS transporters, with a predicted structure containing twelve TMDs divided in half by a large internal loop [2,4]. Among other MFS members, RFC1 demonstrates topology similar to those of the GLUT1 glucose transporter [28] and lactose permease from *Escherichia coli* [29] with N- and C-termini and the largest loop oriented to the cytoplasm. For the lactose permease, the long central loop is required for proper membrane insertion, stability, and transport activity [30]. Studies of several chimeric GLUT1/GLUT5 proteins indicate that the long cytoplasmic loop, together with 7th–12th TMDs, plays a critical role in substrate specificity consistent with the participation of this region in substrate binding [31]. Indirect evidence of participation of the long cytoplasmic loop in transport was also shown in studies in which fragmentation of the 6th–7th TMD connecting loop, after proteolytic digestion of the GLUT1 transporter with papain, was enhanced in the presence of glucose but not sorbitol, indicating that the loop changes conformation upon specific substrate binding [32]. However, interactions between transmembrane domains, but not external or internal hydrophilic regions, appear to have the greatest impact on the maintenance of the three-dimensional structure of glucose and lactose transporters as assessed by coexpression of non-overlapping carrier fragments cut in intracellular loops [33,34].

Deletion of 57 amino acid loop residues resulted in complete inactivation of RFC1, although the truncated protein appeared to be inserted into the plasma membrane. This was in contrast to recent findings that deletion of 20 amino acid residues in the cytoplasmic loop between the 6th and 7th TMDs of lactose permease resulted in defective membrane insertion and decreased protein stability [30]. Thus, this loop in RFC1 is critical to folate binding and/or to maintenance of the tertiary structure. Lesser deletions in the C-terminus region of the loop resulted in partial preservation of carrier function and sensitivity to MTX in transfected lines. Most of the change in 5-CHO-THF transport activity of the Δ17 and Δ31 carriers could be attributed to decreased affinity for this substrate, suggesting that the large intracellular loop takes part in folate

binding. Further, these studies indicate that deletion of 31 amino acids from the C-terminal part of the loop resulted in no greater loss of MTX transport activity than was observed when only 17 amino acids were deleted. In fact, the affinity of 5-CHO-THF for the truncated proteins was decreased less with the Δ31 deletion than with the Δ17 deletion as compared with wild-type RFC1. This implies that the conformational changes in the carrier associated with the Δ17 deletion could be partially compensated for by the loss of additional amino acid residues in the Δ31 mutant and that the length of the long cytoplasmic loop, alone, is not the only crucial element in RFC1 function. Hence, this loop influences the selectivity of substrate binding, likely by carrier conformational changes.

RFC1 functions by an anion exchange mechanism coupled to a transmembrane gradient of organic anions, in particular organic phosphates; however, the carrier region that accounts for this exchange has not been identified. In both murine and human RFC1, substitution of negatively-charged glutamate for positively-charged lysine at position 45 in the first transmembrane domain of RFC1 resulted in the introduction of an obligatory requirement for small inorganic anions for transport function, although it did not appear to be in the anion exchange site [12,15]. In other studies, substitution of serine 309 with phenylalanine or replacement of lysine with leucine at position 404 eliminated the inhibitory effect of chloride on folate influx observed for wild-type RFC1 [13,17]. The present study demonstrates that despite the decreased transport activity in Δ17 and Δ31 mutants, in which up to half of the long cytoplasmic loop was deleted, there was no change in the effects of anion addition (ATP), or anion removal (Cl^-), on transport function as compared with L1210 cells (Fig. 5). Hence, the deleted components of the long cytoplasmic loop are not involved in RFC1 anion exchange.

RFC1 lost all transport activity upon deletion of the C-terminus (68 amino acid residues). This observation is consistent with another study in which a frameshift mutation resulting in the deletion of 61 amino acids at the C-terminus led to a complete loss of RFC1 function and MTX resistance in an L1210 variant (D2) selected by chemical mutagenesis [16]. The inactivation of RFC1 is likely due to instability of the truncated protein since carrier was not detected in the cell lysate. This finding is in contrast to the loss of function observed with a GLUT1 mutant that lacked 37 C-terminus amino acids but was inserted into the plasma membrane [35]. Our finding is also different from the consequence of the C-terminus deletion of the glycine transporter, GLYT1, another member of the MFS family, i.e. impaired trafficking to, or insertion in, the plasma membrane [36]. Hence, deletion of C-terminus of different facilitative transporters has different effects on protein expression, stability, trafficking, and/or functional activity. These findings could be attributed to differences in intrinsic properties of the individual transporters or differences in the lengths of the C-terminus deletions.

Acknowledgment

This work was supported by a grant (CA-82621) from the National Cancer Institute.

References

[1] Sirotnak FM, Tolner B. Carrier-mediated membrane transport of folates in mammalian cells. Annu Rev Nutr 1999;19:91–122.
[2] Dixon KH, Lanpher BC, Chiu J, Kelley K, Cowan KH. A novel cDNA restores reduced folate carrier activity and methotrexate sensitivity to transport deficient cells. J Biol Chem 1994;269:17–20.
[3] Ferguson PL, Flintoff WF. Topological and functional analysis of the human reduced folate carrier by hemagglutinin epitope insertion. J Biol Chem 1999;274:16269–78.
[4] Saier Jr. MH, Beatty JT, Goffeau A, Harley KT, Heijne WH, Huang SC, Jack DL, Jahn PS, Lew K, Liu J, Pao SS, Paulsen IT, Tseng TT, Virk PS. The major facilitator superfamily. J Mol Microbiol Biotechnol 1999;1:257–79.
[5] Goldman ID. The characteristics of the membrane transport of amethopterin and the naturally occurring folates. Ann NY Acad Sci 1971;186:400–22.
[6] Henderson GB, Zevely EM. Structural requirements for anion substrates of the methotrexate transport system of L1210 cells. Arch Biochem Biophys 1983;221:438–46.
[7] Yang C-H, Sirotnak FM, Dembo M. Interaction between anions and the reduced folate/methotrexate transport system in L1210 cell plasma membrane vesicles: directional symmetry and anion specificity for differential mobility of loaded and unloaded carrier. J Membr Biol 1984;79:285–92.
[8] Tse A, Brigle K, Taylor SM, Moran RG. Mutations in the reduced folate carrier gene which confer dominant resistance to 5,10-dideazatetrahydrofolate. J Biol Chem 1998;273:25953–60.
[9] Roy K, Tolner B, Chiao JH, Sirotnak FM. A single amino acid difference within the folate transporter encoded by the murine RFC-1 gene selectively alters its interaction with folate analogues: implications for intrinsic antifolate resistance and directional orientation of the transporter within the plasma membrane of tumor cells. J Biol Chem 1998;273:2526–31.
[10] Brigle KE, Spinella MJ, Sierra EE, Goldman ID. Characterization of a mutation in the reduced folate carrier in a transport defective L1210 murine leukemia cell line. J Biol Chem 1995;270:22974–9.
[11] Zhao R, Assaraf YG, Goldman ID. A reduced carrier mutation produces substrate-dependent alterations in carrier mobility in murine leukemia cells and methotrexate resistance with conservation of growth in 5-formyltetrahydrofolate. J Biol Chem 1998;373:7873–9.
[12] Zhao R, Assaraf YG, Goldman ID. A mutated murine reduced folate carrier (RFC1) with increased affinity for folic acid, decreased affinity for methotrexate, and an obligatory anion requirement for transport function. J Biol Chem 1998;273:19065–71.
[13] Zhao R, Gao F, Goldman ID. Discrimination among reduced folates and methotrexate as transport substrates by a phenylalanine substitution for serine within the predicted eighth transmembrane domain of the reduced folate carrier. Biochem Pharmacol 1999;58:1615–24.
[14] Zhao R, Gao F, Wang PJ, Goldman ID. Role of the amino acid 45 residue in reduced folate carrier function and ion-dependent transport as characterized by site-directed mutagenesis. Mol Pharmacol 2000; 57:317–23.
[15] Jansen G, Mauritz R, Drori S, Sprecher H, Kathmann I, Bunni M, Priest DG, Noordhuis P, Schornagel JH, Pinedo HM, Peters GJ, Assaraf YG. A structurally altered human reduced folate carrier with increased folic acid transport mediates a novel mechanism of antifolate resistance. J Biol Chem 1998;273:30189–98.

[16] Zhao R, Sharina IG, Goldman ID. Pattern of mutations that results in loss of reduced folate carrier function under antifolate selective pressure augmented by chemical mutagenesis. Mol Pharmacol 1999;56:68–76.
[17] Sharina IG, Zhao R, Wang Y, Babani S, Goldman ID. Mutational analysis of the functional role of conserved arginine and lysine residues in transmembrane domains of the murine reduced folate carrier. Mol Pharmacol 2001;59:1022–8.
[18] Fry DW, Yalowich JC, Goldman ID. Rapid formation of poly-γ-glutamyl derivatives of methotrexate and their association with dihydrofolate reductase as assessed by high pressure liquid chromatography in the Ehrlich ascites tumor cell *in vitro*. J Biol Chem 1982;257: 1890–6.
[19] Kuroki T. Colony formation of mammalian cells on agar plates and its application to Lederberg's replica plating. Exp Cell Res 1973;80:55–62.
[20] Zhao R, Gao F, Liu L, Goldman ID. The reduced folate carrier in L1210 murine leukemia cells is a 58 kDa protein. Biochim Biophys Acta 2000;1466:7–10.
[21] Henderson GB, Zevely EM. Affinity labeling of the 5-methyltetrahydrofolate/methotrexate transport protein of L1210 cells by treatment with an *N*-hydroxysuccinimide ester of [^{3}H]methotrexate. J Biol Chem 1984;259:4558–62.
[22] Zhao R, Seither R, Brigle KE, Sharina IG, Wang PJ, Goldman ID. Impact of overexpression of the reduced folate carrier (RFC1), an anion exchanger, on concentrative transport in murine L1210 leukemia cells. J Biol Chem 1997;272:21207–12.
[23] Higgins DG, Sharp PM. CLUSTAL: a package for performing multiple sequence alignment on a microcomputer. Gene 1988;73:237–44.
[24] Zhao R, Russell RG, Wang Y, Liu L, Gao F, Kneitz B, Edelman W, Goldman ID. Rescue of embryonic lethality in reduced folate carrier-deficient mice by maternal folic acid supplementation reveals early neonatal failure of hematopoietic organs. J Biol Chem 2001;276: 10224–8.
[25] Gorlick R, Goker E, Trippett T, Steinherz P, Elisseyeff Y, Mazumdar M, Flintoff WF, Bertino JR. Defective transport is a common mechanism of acquired methotrexate resistance in acute lymphocytic leukemia and is associated with decreased reduced folate carrier expression. Blood 1997;89:1013–8.
[26] Matherly LH, Taub JW, Ravindranath Y, Proefke SA, Wong SC, Gimotty P, Buck S, Wright JE, Rosowsky A. Elevated dihydrofolate reductase and impaired methotrexate transport as elements in methotrexate resistance in childhood acute lymphoblastic leukemia. Blood 1995;85:500–9.
[27] Sierra EE, Goldman ID. Recent advances in understanding of the mechanism of membrane transport of folates and antifolates. Semin Oncol 1999;26(Suppl 6):11–23.
[28] Hresko RC, Kruse M, Strube M, Mueckler M. Topology of the GLUT1 glucose transporter deduced from glycosylation scanning mutagenesis. J Biol Chem 1994;269:20482–8.
[29] Kaback HR, Wu J. From membrane to molecule to the third amino acid from the left with a membrane transport protein. Q Rev Biophys 1997;30:333–64.
[30] Weinglass AB, Kaback HR. The central cytoplasmic loop of the major facilitator superfamily of transport proteins governs efficient membrane insertion. Proc Natl Acad Sci USA 2000;97:8938–43.
[31] Inukai K, Katagiri H, Takata K, Asano T, Anai M, Ishihara H, Nakazaki M, Kikuchi M, Yazaki Y, Oka Y. Characterization of rat GLUT5 and functional analysis of chimeric proteins of GLUT1 glucose transporter and GLUT5 fructose transporter. Endocrinology 1995;136:4850–7.
[32] Asano T, Katagiri H, Tsukuda K, Lin JL, Ishihara H, Inukai K, Yazaki Y, Oka Y. Glucose binding enhances the papain susceptibility of the intracellular loop of the GLUT1 glucose transporter. FEBS Lett 1992;298:129–32.
[33] Cope DL, Holman GD, Baldwin SA, Wolstenholme AJ. Domain assembly of the GLUT1 glucose transporter. Biochem J 1994; 300:291–4.
[34] Zen KH, McKenna E, Bibi E, Hardy D, Kaback HR. Expression of lactose permease in contiguous fragments as a probe for membrane-spanning domains. Biochemistry 1994;33:8198–206.
[35] Oka Y, Asano T, Shibasaki Y, Lin JL, Tsukuda K, Katagiri H, Akanuma Y, Takaku F. C-terminal truncated glucose transporter is locked into an inward-facing form without transport activity. Nature 1990;345:550–3.
[36] Olivares L, Aragon C, Gimenez C, Zafra F. Carboxyl terminus of the glycine transporter GLYT1 is necessary for correct processing of the protein. J Biol Chem 1994;269:28400–4.